Brief communication: The anomalous winter 2019 sea ice conditions in McMurdo Sound, Antarctica

Greg H. Leonard[1], Kate E. Turner[2, 3], Maren E. Richter[2], Maddy S. Whittaker[2], and Inga J. Smith[2]

[1]National School of Surveying, University of Otago, Dunedin, New Zealand
[2]Department of Physics, University of Otago, Dunedin, New Zealand
[3]National Institute of Water and Atmospheric Research, Wellington, New Zealand

Correspondence: Greg Leonard (greg.leonard@otago.ac.nz)

Abstract.

McMurdo Sound sea ice can generally be partitioned into two regimes: (1) a stable fast-ice cover, forming south of approximately 77.6° S around March / April, then breaking out the following January / February; and, (2) a more dynamic region north of 77.6° S that the McMurdo Sound and Ross Sea polynyas regularly impact. In 2019, a stable fast-ice cover formed unusually late due to repeated break-out events. We analyse the 2019 sea-ice conditions and relate them to southerly wind events using a ~~Katabatic Wind Index (KWI~~Modified Storm Index (MSI). We find there is a strong correlation between the timing of break-out events and several unusually large ~~KWI~~ MSI events.

1 Introduction

The sea-ice cover in McMurdo Sound can generally be partitioned into two regimes: (1) a stable fast-ice cover occupying the southeastern and western parts of the ~~Sound~~sound, south of a latitude of approximately 77.6° S; and, (2) a more dynamic region in the central part of the ~~Sound~~sound. Regime (1) is primarily made up of first-year sea ice that forms around late March / early April and typically breaks out in January / February of the following year (Kim et al., 2018) whereas Regime (2) is impacted by the McMurdo Sound Polynya (MSP) and Ross Sea Polynya (RSP) (Brett et al., 2020). The boundary between the regimes is influenced by such factors as ~~ice-shelf ocean~~ ice-shelf–ocean interactions, ocean circulation ~~(e.g. Hughes et al., 2014; Robinson et al., 2014)~~ (e.g., Hughes et al., 2014; Robinson et al., 2014) and the location of grounded icebergs ~~(e.g. Brunt et al., 2006; Robinson and Williams, 2012)~~ (e.g., Brunt et al., 2006; Robinson and Williams, 2012) and can vary on annual timescales.

McMurdo Sound logistical and scientific ~~sea ice~~ sea-ice operations depend on the formation of a stable fast-ice cover over the winter months that persists through to late December / early January. In 2019, the formation of the ~~fast ice~~ stable fast-ice cover was significantly delayed, impacting operations for both the New Zealand and the United States of America Antarctic programmes. Impacts included: the non-establishment of a ~~sea ice~~ sea-ice route to Marble Point (a cache for helicopter fuel and other supplies); a reduction in the number of ~~sea ice~~ sea-ice scientific field sites; and a two-month delay in the deployment of the University of Otago ~~sea ice~~ sea-ice mass balance station.

We are not aware of any studies directly investigating the causes of delayed freeze-up of sea ice in McMurdo Sound. Kim et al. (2018) found that in years with higher mean annual wind speeds, the fast ice generally retreated earlier in the season, however, that study did not look at the impact of individual events on ~~break up~~ break-up and retreat. At the event level, investigations by Banwell et al. (2017) into causes of the calving of the McMurdo Ice Shelf in 2016 suggested that strong (>10 m s^{-1}) winds from the south and west contributed to the large ~~fast ice~~ fast-ice break-up event that preceded the calving event. Brunt et al. (2006) investigated sea-ice break-out events in the southwest Ross Sea between 1996 and 2005 using satellite imagery and automatic weather station data. They found that break-out events were correlated with a dimensionless "storm index", defined as the product of ~~low pressure~~ low-pressure anomalies and anomalous temperature (lower temperatures in summer and higher temperatures in winter).

In this brief communication we investigate the linkages between ~~enhanced MSP activity,~~ more frequent opening of the MSP due to increased ~~winter storm frequency and intensity~~frequency of intense winter storms, and the delay in the formation of a stable ~~fast ice~~ fast-ice cover in 2019. We quantify winter storm intensity by introducing a ~~Katabatic Wind Index (KWI~~Modified Storm Index (MSI) that is based on the approach of Brunt et al. (2006), but here is applied to individual events as opposed to seasonal trends. The 2019 McMurdo Sound ~~sea ice~~ sea-ice cover properties are derived from a combination of manual assessment of Synthetic Aperture Radar (SAR) and MODIS derived ~~ice surface~~ ice-surface temperatures and analysing ~~sea ice~~ sea-ice concentrations generated by the ARTIST Sea Ice (ASI) algorithm (Spreen et al., 2008).

2 McMurdo Sound sea ice characteristics

The edge of the stable fast-ice cover typically extends west-to-east from a band of fast ice ~20 km wide along the Victoria Land Coast to Cape Royds, Ross Island (see Figure 1a). To investigate when this ~~sea ice~~ sea-ice cover forms, we analysed the Fraser et al. (2020) circum-Antarctic land-fast sea-ice distribution data set derived from cloud-free, ~~14-day~~ 15-day composites of satellite visible–thermal infrared imagery. This data set covers the period from March 2000 to February 2018 and includes the time period when the sea ice in McMurdo Sound was strongly impacted by the presence of very large, tabular icebergs (e.g., C-19 and B-15A) at the mouth of the ~~Sound~~sound.

From 2001 to 2005, the sea ice (Brunt et al., 2006) and ocean circulation (Robinson and Williams, 2012) in McMurdo Sound were directly influenced by these icebergs, leading to the presence of multi-year ice and anomalously large ~~sea ice extents that biased~~ sea-ice extents that influenced the studies of Brunt et al. (2006) and Kim et al. (2018). The effects on the fast ice in McMurdo Sound were felt for several years after the icebergs exited the region, as evidenced by the fact that a multi-year ~~fast ice covered~~ fast-ice cover remained in place in the southern part of the ~~Sound~~ sound until February 2011. Therefore, the ~~fast ice~~ fast-ice extents for these years (2001 – 2011) have been excluded from ~~our analysis.~~ this analysis.

In years that were not iceberg-affected (2000; 2012 – 2017), the ~~fast ice~~ fast-ice cover in the ~~Sound~~ sound generally reached a minimum in mid-March where it typically ~~recedes~~ receded into a few pockets along the Victoria Land Coast in the west of the ~~Sound~~sound, around the Erebus Glacier Tongue along the west coast of Ross Island and into a wedge-shaped area between the tip of the Hut Point Peninsula on Ross Island and the McMurdo Ice Shelf. The ~~fast ice~~ fast-ice cover south of 77.6° S typically ~~re-forms~~ re-formed sometime between mid-March and mid-April, with the exception of 2012, where it did not form until around the end of June. This is contrasted with 2019 when a stable fast-ice cover did not form until late July.

2.1 2019 sea ice conditions

An analysis of radar (Sentinel-1 SAR) imagery and MODIS 1 km resolution ~~ice surface temperatures~~ Ice Surface Temperature (IST) (Hall and Riggs, 2015a, b) during the period April – July 2019 revealed an unusually large number of MSP events ~~, and the~~ (a "polynya event" being defined here as a polynya opening that impacts on the previously established fast-ice cover). The frequency and intensity of these events ~~impacted the~~ resulted in the eroding of the fast-ice cover ~~by repeatedly eroding it~~ all the way back to the edge of the ice shelf, ~~which is~~ ~30 km farther south than 77.6° S. ~~Prior to the events, MODIS ice surface temperatures typically showed warming in the east of the Sound, suggesting a fractional ice cover and removal of first-year ice, consistent with activation of the MSP. From 15~~The SAR imagery used in this study were a combination of Extra Wide (EW) medium resolution imagery (40 m pixel size) and Interferometric Wide (IW) high resolution mode imagery (10 m pixel size resampled to 40 m pixel size for this study). From 1 April to 1 September, eight large MSP events were observed in SAR images, ~~including 21~~ three of which are shown in Figure 1b – d (21 May, 25 ~~-~~June and 8 ~~July(reference Figure 1b – d)and 19 and 21 April, 6 and 8 May and 10 June (not shown)~~ July). Prior to the events, MODIS IST pixels in the east of the sound typically show increased temperature values, although we are unable to determine whether these higher ISTs resulted from increased ice surface temperatures or sea ice within these pixels being dynamically broken-up and advected northward due to wind forcing (hence exposing underlying warm ocean water), or a combination of the two. Due to this, and the well-documented issues with cloud masking in the MODIS IST product (e.g., Mäkynen and Karvonen, 2017), we used MODIS IST as a secondary source to corroborate SAR observations rather than the primary source to define fast-ice break-out events. However, by qualitatively comparing spatial patterns of elevated IST pixels with coincident (when available) SAR imagery during break-out events, we observed that elevated IST pixels typically occur in areas in the eastern sound where the MSP was active, suggesting that increased ISTs are at least partially a result of polynya activity.

~~Manually identified~~ Manually-identified fast-ice break-out events were contextualised with ~~sea ice~~ sea-ice concentrations derived from the ARTIST Sea Ice (ASI) algorithm (Spreen et al., 2008). Figure 1e and f show sea ice concentrations for the late-June and mid-July event, respectively. The ARTIST ~~landmask~~ land mask extends up to ~15 km into the southern ~~Sound, hence sea ice~~ sound, hence sea-ice concentrations cannot be determined in this area. Due to the challenges of discriminating between thin ice and fast ice in passive microwave satellite brightness temperatures, (e.g., Tamura et al., 2007, 2008; Nihashi and Ohshima, 2015), we do not attempt to quantify polynya area from the ARTIST derived sea-ice concentrations. Instead, we introduce a daily sea-ice fraction metric (see Section 4) to characterise regional changes in sea-ice extent within McMurdo Sound. In comparing Figure 1c to Figure 1e it can be seen that the late-June event broke up the ~~fast ice~~ fast-ice cover all the way back to the edge of the ice shelf, but this has not been fully captured in the ARTIST ~~sea ice concentration~~sea-ice concentration, due to the land mask. This delayed the impact of the late-June event on the ARTIST ~~sea ice~~ sea-ice concentrations by a couple of days, which will be discussed further in Section 4.

3 Characterisation of winter storms

~~Strong wind events in this region are dominated by~~

Strong surface-wind events in McMurdo Sound can develop when southerly katabatic and barrier winds that flow off the Ross Ice Shelf ~~(e.g. Coggins et al., 2013; Parish et al., 2006) and are channeled into McMurdo Sound. These~~ (e.g., Coggins et al., 2013; Parish et interact with synoptic-scale low pressure systems forming to the east of Ross Island. In winter, these winds are typically ~~connected to warm temperatures and~~ associated with low air pressure ~~(e.g. Coggins et al., 2013; Chenoli et al., 2013). During winter, higher~~ and warm near-surface air temperatures. (e.g., Coggins et al., 2013; Chenoli et al., 2013). The relative warmth of the surface winds results from high wind speeds (above 4 – 6 m s^{-1}) ~~increase the~~ increasing the vertical mixing between the relatively cold surface inversion layer over the ice shelf and the warmer overlying atmosphere (Cassano et al., 2016) ~~. The increase in temperature may also be partly influenced by the Föhn effect, whereby katabatic winds from the Transantarctic Mountains, one of the sources of southerly winds on the Ross Ice Shelf (Parish et al., 2006), experience adiabatic warming. Southerly~~ and warm, marine air being incorporated from the synoptic-scale lows. Dale et al. (2017) found that southerly wind events in the Ross Sea are correlated ~~to sea ice~~ with low sea-ice concentration and the opening of the Ross Sea Polynya (RSP)~~(Dale et al., 2017) and in~~ , which they attributed to strong winds causing northward advection of sea ice. They also observed that a rapid decrease in sea-ice concentration during a strong wind event was followed by a more gradual recovery. Ebner et al. (2013) undertook mesoscale atmospheric model simulations coupled with a sea-ice–ocean model to investigate the formation of polynyas in the coastal region of Coats Land, which is an area strongly affected by katabatic winds. They identified linkages between a pressure gradient force composed of a katabatic and a synoptic component, offshore wind regimes and polynya area. Here we examine the ~~following we will examine this relationship for the McMurdo Sound Polynya in~~ relationship between strong surface-wind events in McMurdo Sound and the opening of the MSP in the winter of 2019.

~~The wind climatologies~~ The available observational wind data for Scott Base (Figure 2) show that the months ~~leading to the freeze-up of~~ preceding the formation of a stable fast-ice cover in McMurdo Sound in 2019 were characterised by particularly strong southerly winds. Columns 1 and 2 of Figure 2 indicate that southerly winds for these months in 2019 were more frequent, and in the case of the June and July months, stronger, than the average of previous years (1997 – 2018). Columns 3 and 4 further highlight periods of particularly strong (up to 30 m s^{-1}) winds during June and July, well above their climatological 90th percentiles, (10.3 and 10.0 m s^{-1}, respectively). These strong wind events can be seen in Figure 3c and d, corresponding with the timing of the fast-ice break-out events as identified through satellite imagery.

To investigate this further, following the approach of Brunt et al. (2006), we used hourly 20 m air temperature and ~~atmospheric pressure~~ mean sea-level pressure (MSLP) data from the Scott Base weather station to construct a dimensionless ~~Katabatic Wind Index (KWI).~~ Modified Storm Index (MSI). Mean hourly climatologies of temperature and MSLP were constructed by applying a three-day smoothing window to the mean of hourly observations from 2002 – 2018. As the period of interest spans only the winter months, we define the ~~KWI~~ MSI as the product of ~~the~~ normalised positive air temperature and negative ~~mean sea level pressure~~ MSLP anomalies, as calculated in relation to ~~the climatological mean. This index~~ their climatological means. The MSI was then smoothed over a 12-hour window. The index, and the corresponding air temperature and ~~mean sea level pressure~~ MSLP data, are shown in Figure 3.

As defined by this index, in the period ~~15~~1 April to 1 September, three large ~~katabatic wind events~~ storm events (MSI > 0.20) leading to MSP ~~activations~~ openings occurred in mid-June, late-June and mid-July of 2019, again coincident with times when large break-out events were identified ~~. Two smaller events occurred in May. There were also several KWI events~~in ~~August that did not lead to large~~ the Sentinel-1 SAR imagery. Smaller events can also be seen in the preceding months, largely concurrent with Sentinel-1 implied break-out events. After freeze-in occurred in late July, the storm events were not not strong enough to lead to significant break-out ~~events.~~ of the fast ice.

4 Impact of mid-winter southerly wind events on the 2019 ~~fast ice~~ fast-ice cover

To quantify the effect of ~~katabatic~~ these storm events on the 2019 ~~sea ice~~ sea-ice cover, we first computed a daily ~~sea ice fraction~~ sea-ice fraction (which we assigned to mid-day) for McMurdo Sound for the period ~~15~~1 April to 1 September over the entire ARTIST record (2013 – 2019). The ~~sea ice~~ sea-ice fraction was calculated by summing the number of pixels within the bounds of the red box shown in Figure 1a where the ~~sea ice~~ sea-ice concentration was 15 % or greater (a typical threshold used to determine sea ice extent) and dividing by the total number of pixels (n = 553), excluding land masked pixels. This method was chosen in preference to computing an average sea ice concentration as it is better suited to quantifying changes in sea ice extent, which we equate generally to changes in the fast-ice cover in the sound.

~~The sea ice~~ The sea-ice fractions for the years 2013 – 2019 are shown in Figure 3a, with the 2019 data indicated by a thick black line. It can be clearly seen that the timing of low (< ~~0.8) sea ice~~ 0.80) sea-ice fraction events correspond with identified ~~sea ice~~ sea-ice break-out events, even though the ~~sea ice~~ sea-ice fraction is likely underestimating the amount of open water due to the protrusion of the ARTIST land mask into the southern reaches of the ~~Sound~~sound. An example of this is the late-June event (reference Figure 1c) where the ~~sea ice~~ sea-ice fraction decrease lags the ~~KWI and the manually~~ MSI and the Sentinel-1 identified break-out event by a couple of days. This break-out event was characterised by the MSP first ~~activating~~ opening just off the edge of the ice shelf (which is masked out in the ARTIST sea ice concentrations) before expanding northward, whereas in other events the polynya tends to be centred farther to the ~~North~~north. The 2019 record stands apart from other years, both in terms of the number of low ~~ice fraction events overall , and particularly during the months of~~ ice-fraction events overall and it being the only year where ice-fractions in June and July ~~where it was the only year in the time series to record low sea ice fraction events during these months.~~ decreased below 0.75.

5 Discussion

The strength of a sea-ice cover is impacted by factors such as its thickness, internal temperature, salinity and porosity (Timco and Weeks, 20 . As these parameters, as well as ocean properties such as surface currents and waves, were not observed in this study, we are only able to evaluate impacts on fast-ice cover integrity from wind forcing, and not from other drivers such as thermal and ocean forcing, and hence are unable to unequivocally identify the mechanism for a particular break-out event. However, we note that Kim et al. (2018) did not find a significant relationship between sea-ice temperature and break-out in their study, and we did not observe any correlation between tidal state and the 2019 break-out events in this study. Furthermore, the entire water column in McMurdo Sound during winter is conditioned by supercooled water flowing out from the McMurdo Ice Shelf cavity (Leonard et al., 2006), resulting in it being nearly isothermal and very close to its freezing point (Lewis and Perkin, 1985; Mahoney et al., 2 , suggesting that any water upwelled from the opening of the MSP would not cause melting of the fast-ice cover. Finally, we would not anticipate wave action playing a significant role in breaking up the fast-ice cover due to the absence of upstream fetch associated with the southerly winds.

Our analysis implies that the stability of the McMurdo Sound fast-ice cover south of 77.6° S is potentially vulnerable to storm events from late spring to mid-winter. The fast-ice cover tends to be more responsive to storm events in April and May, presumably because the ice cover is still relatively thin and warm and lacks the strength to resist the drag force from the southerly winds. The ~~KWI climatology indicates that the frequency and intensity of~~ MSI climatology suggests the frequency of intense southerly storms tends to decrease in the months of June and July. This typically allows the ~~fast ice~~ fast-ice cover to thicken and gain strength during these months, which means that it is sufficiently strong to remain intact when the southerly winds increase, on average, later in the year.

~~In~~ However, in 2019, the frequency ~~and intensity of~~ of intense storms in June and July ~~were~~ was such that the fast-ice cover was too weak to withstand the southerly winds and was broken up and advected northwards on three separate occasions. Immediately following the mid-July event, the ~~KWI indicates~~ MSI and wind data indicate a more quiescent weather pattern, allowing the ~~fast ice~~ fast-ice cover to reform and presumably gain strength. ~~The KWI increases~~

The MSI increased again in mid-August, however, the fast-ice cover south of 77.6° S ~~is~~ was now able to resist the southerly wind stress and ~~stays~~ stayed fixed in place for the remainder of the growth season. ~~This result is generally consistent with the findings of Brett et al. (2020) who described the impact of increased southerly winds in winter in 2011 and 2017 on McMurdo Sound fast ice.~~ Brett et al. (2020) explored reasons for an anomalously extensive fast-ice cover in McMurdo Sound in 2016 and related relatively low activity of the RSP and MSP over winter with calmer conditions that led to largely undisturbed sea ice growth in 2016. Here, we have observed the opposite scenario where a more active MSP, resulting from an increase in the frequency of intense winter storms, has resulted in an anomalously dynamic fast-ice cover. Both studies clearly illustrate the impact winter storms have on the fast-ice cover in McMurdo Sound.

6 Conclusions

Here we have investigated the impact of winter storms on the stability of an Antarctic fast-ice cover. Our key finding is that an increase in the frequency of intense winter storms in 2019 resulted in a delayed formation of a stable fast-ice cover in McMurdo

Sound. This case study is one of a few to investigate the stability of a fast-ice cover, an area that is in need of future research to improve the parameterisation of fast-ice processes in large-scale sea ice models such as CICE and LIM. McMurdo Sound is a well-suited location for fast ice studies with its extensive and accessible (due to its proximity to the US McMurdo Station and New Zealand Scott Base) fast-ice cover. It is also a unique environment in that it is a relatively deep embayment that experiences cold water outflow from an adjacent ice shelf cavity that leads to the formation of a sub-ice platelet layer, making it an ideal location to investigate ice-shelf–ocean–fast-ice feedbacks along the Antarctic coastal margin.

Data availability. Scott Base weather station data are available from https://cliflo.niwa.co.nz/. Sentinel-1 SAR images were accessed through the Alaska Satellite Facility DAAC, at https://search.asf.alaska.edu/ and MODIS images were accessed through https://urs.earthdata.nasa.gov. ARTIST sea ice concentration data accessed from the University of Bremen data archive at https://seaice.uni-bremen.de/data/. Circum-Antarctic landfast sea ice extent data accessed from the Australian Antarctic Data Centre at https://data.aad.gov.au/metadata/records/AAS_4116_Fraser_fastice_circumantarctic.

Author contributions. GHL had the initial idea for this study and analysed the satellite images/products. KET analysed the climatological data in reference to the break-out events and designed the MSI. MER analysed the Scott Base weather station climatology. MSW identified break out events in 2019 from SAR and MODIS images. GHL, KET, MER and IJS discussed the results and prepared the manuscript. All authors contributed to the final review of the manuscript.

Competing interests. There are no competing interests.

Acknowledgements. This paper is an output from the project "Supercooling measurements under ice shelves" supported by the Marsden Fund Council from Government funding, administered by the Royal Society of New Zealand (Marsden Fund contract number MFP-UOO1825). MSW was supported on a summer scholarship from that project, and IJS and GHL's time was supported by that project. MER is supported by a University of Otago Doctoral Scholarship and an Antarctica New Zealand Sir Robin Irvine Post-Graduate Scholarship. The authors are very grateful to Alex Fraser and an anonymous reviewer for their constructive comments. The authors further appreciate a discussion with David Bromwich regarding the wind regime in McMurdo Sound.

References

Banwell, A. F., Willis, I. C., Macdonald, G. J., Goodsell, B., Mayer, D. P., Powell, A., and Macayeal, D. R.: Calving and rifting on the McMurdo Ice Shelf, Antarctica, Annals of Glaciology, 58, 78–87, https://doi.org/10.1017/aog.2017.12, 2017.

Brett, G. M., Irvin, A., Rack, W., Haas, C., Langhorne, P. J., and Leonard, G. H.: Variability in the Distribution of Fast Ice and the Sub-ice Platelet Layer Near McMurdo Ice Shelf, Journal of Geophysical Research: Oceans, 125, e2019JC015 678, https://doi.org/10.1029/2019JC015678, 2020.

Brunt, K. M., Sergienko, O., and MacAyeal, D. R.: Observations of unusual fast-ice conditions in the southwest Ross Sea, Antarctica: preliminary analysis of iceberg and storminess effects, Annals of Glaciology, 44, 183–187, https://doi.org/10.3189/172756406781811754, 2006.

Cassano, J. J., Nigro, M. A., and Lazzara, M. A.: Characteristics of the near-surface atmosphere over the Ross Ice Shelf, Antarctica, Journal of Geophysical Research: Atmospheres, 121, 3339–3362, https://doi.org/10.1002/2015JD024383, 2016.

Chenoli, S. N., Turner, J., and Samah, A. A.: A climatology of strong wind events at McMurdo station, Antarctica, International journal of climatology, 33, 2667–2681, https://doi.org/10.1002/joc.3617, 2013.

Coggins, J. H. J., McDonald, A., and Jolly, B.: Synoptic climatology of the Ross Ice Shelf and Ross Sea region of Antarctica: *k*-means clustering and validation, International Journal of Climatology, 34, 2330–2348, https://doi.org/10.1002/joc.3842, 2013.

Dale, E. R., McDonald, A. J., Coggins, J. H. J., and Rack, W.: Atmospheric forcing of sea ice anomalies in the Ross Sea polynya region., The Cryosphere, 11, 267–280, https://doi.org/10.5194/tc-11-267-2017, 2017.

Ebner, L., Heinemann, G., Haid, V., and Timmermann, R.: Katabatic winds and polynya dynamics at Coats Land, Antarctica, Antarctic Science, 26, 309–326, https://doi.org/10.1017/S0954102013000679, 2013.

Fraser, A. D., Massom, R. A., Ohshima, K. I., Willmes, S., Kappes, P. J., Cartwright, J., and Porter-Smith, R.: High-resolution mapping of circum-Antarctic landfast sea ice distribution, 2000–2018, Earth System Science Data Discussions, 12, 1–18, https://doi.org/10.5194/essd-12-2987-2020, 2020.

Hall, D. K. and Riggs, G. A.: MODIS/Aqua Sea Ice Extent 5-Min L2 Swath 1km, Version 6. [Ice Temperature]. Boulder, Colorado USA. NASA National Snow and Ice Data Center Distributed Active Archive Center., https://doi.org/10.5067/MODIS/MYD29.006, 2015a.

Hall, D. K. and Riggs, G. A.: MODIS/Terra Sea Ice Extent 5-Min L2 Swath 1km, Version 6. [Ice Temperature]. Boulder, Colorado USA. NASA National Snow and Ice Data Center Distributed Active Archive Center., https://doi.org/10.5067/MODIS/MYD29.006, 2015b.

Hughes, K. G., Langhorne, P. J., Leonard, G. H., and Stevens, C. L.: Extension of an Ice Shelf Water plume model beneath sea ice with application in McMurdo Sound, Antarctica, Journal of Geophysical Research: Oceans, 119, 8662–8687, https://doi.org/10.1002/2013jc009411, 2014.

Kim, S., Saenz, B., Scanniello, J., Daly, K., and Ainley, D.: Local climatology of fast ice in McMurdo Sound, Antarctica, Antarctic Science, 30, 125–142, https://doi.org/10.1017/s0954102017000578, 2018.

Lazzara, M. A., Weidner, G. A., Keller, L. M., Thom, J. E., and Cassano, J. J.: Antarctic automatic weather station program: 30 years of polar observations, Bulletin of the American Meteorological Society, 93, 1519–1537, https://doi.org/10.1175/BAMS-D-11-00015.1, 2012.

Leonard, G. H., Purdie, C. R., Langhorne, P. J., Haskell, T. G., Williams, M. J. M., and Frew, R. D.: Observations of platelet ice growth and oceanographic conditions during the winter of 2003 in McMurdo Sound, Antarctica, Journal of Geophysical Research-Oceans, 111, https://doi.org/10.1029/2005jc002952, 2006.

Lewis, E. L. and Perkin, R. G.: The winter oceanography of McMurdo Sound, Antarctica, in: Oceanology of the Antarctic Continental Shelf, edited by Jacobs, S. S., vol. 43 of *Antarctic Research Series*, pp. 145–165, AGU, Washington, DC, https://doi.org/10.1029/AR043p0145, 1985.

Mahoney, A. R., Gough, A. J., Langhorne, P. J., Robinson, N. J., Stevens, C. L., Williams, M. M. J., and Haskell, T. G.: The seasonal appearance of ice shelf water in coastal Antarctica and its effect on sea ice growth, Journal of Geophysical Research-Oceans, 116, https://doi.org/10.1029/2011jc007060, 2011.

Mäkynen, M. and Karvonen, J.: MODIS Sea Ice Thickness and Open Water–Sea Ice Charts over the Barents and Kara Seas for Development and Validation of Sea Ice Products from Microwave Sensor Data, Remote Sensing, 9, https://doi.org/10.3390/rs9121324, https://www.mdpi.com/2072-4292/9/12/1324, 2017.

Nihashi, S. and Ohshima, K. I.: Circumpolar Mapping of Antarctic Coastal Polynyas and Landfast Sea Ice: Relationship and Variability, Journal of Climate, 28, 3650 – 3670, https://doi.org/10.1175/JCLI-D-14-00369.1, https://journals.ametsoc.org/view/journals/clim/28/9/jcli-d-14-00369.1.xml, 2015.

Parish, T. R., Cassano, J. J., and Seefeldt, M. W.: Characteristics of the Ross Ice Shelf air stream as depicted in Antarctic Mesoscale Prediction System simulations, Journal of Geophysical Research: Atmospheres, 111, https://doi.org/10.1029/2005JD006185, 2006.

Robinson, N. J. and Williams, M. J. M.: Iceberg-induced changes to polynya operation and regional oceanography in the southern Ross Sea, Antarctica, from in situ observations, Antarctic Science, 24, 514–526, https://doi.org/10.1017/s0954102012000296, 2012.

Robinson, N. J., Williams, M. J. M., Stevens, C. L., Langhorne, P. J., and Haskell, T. G.: Evolution of a supercooled Ice Shelf Water plume with an actively growing subice platelet matrix, Journal of Geophysical Research: Oceans, 119, 3425–3446, https://doi.org/10.1002/2013JC009399, 2014.

Spreen, G., Kaleschke, L., and Heygster, G.: Sea ice remote sensing using AMSR-E 89-GHz channels, Journal of Geophysical Research: Oceans, 113, https://doi.org/10.1029/2005JC003384, 2008.

Tamura, T., Ohshima, K. I., Markus, T., Cavalieri, D. J., Nihashi, S., and Hirasawa, N.: Estimation of Thin Ice Thickness and Detection of Fast Ice from SSM/I Data in the Antarctic Ocean, Journal of Atmospheric and Oceanic Technology, 24, 1757 – 1772, https://doi.org/10.1175/JTECH2113.1, https://journals.ametsoc.org/view/journals/atot/24/10/jtech2113_1.xml, 2007.

Tamura, T., Ohshima, K. I., and Nihashi, S.: Mapping of sea ice production for Antarctic coastal polynyas, Geophysical Research Letters, 35, https://doi.org/https://doi.org/10.1029/2007GL032903, https://agupubs.onlinelibrary.wiley.com/doi/abs/10.1029/2007GL032903, 2008.

Timco, G. W. and Weeks, W. F.: A review of the engineering properties of sea ice, Cold regions science and technology, 60, 107–129, https://doi.org/10.1016/j.coldregions.2009.10.003, 2010.

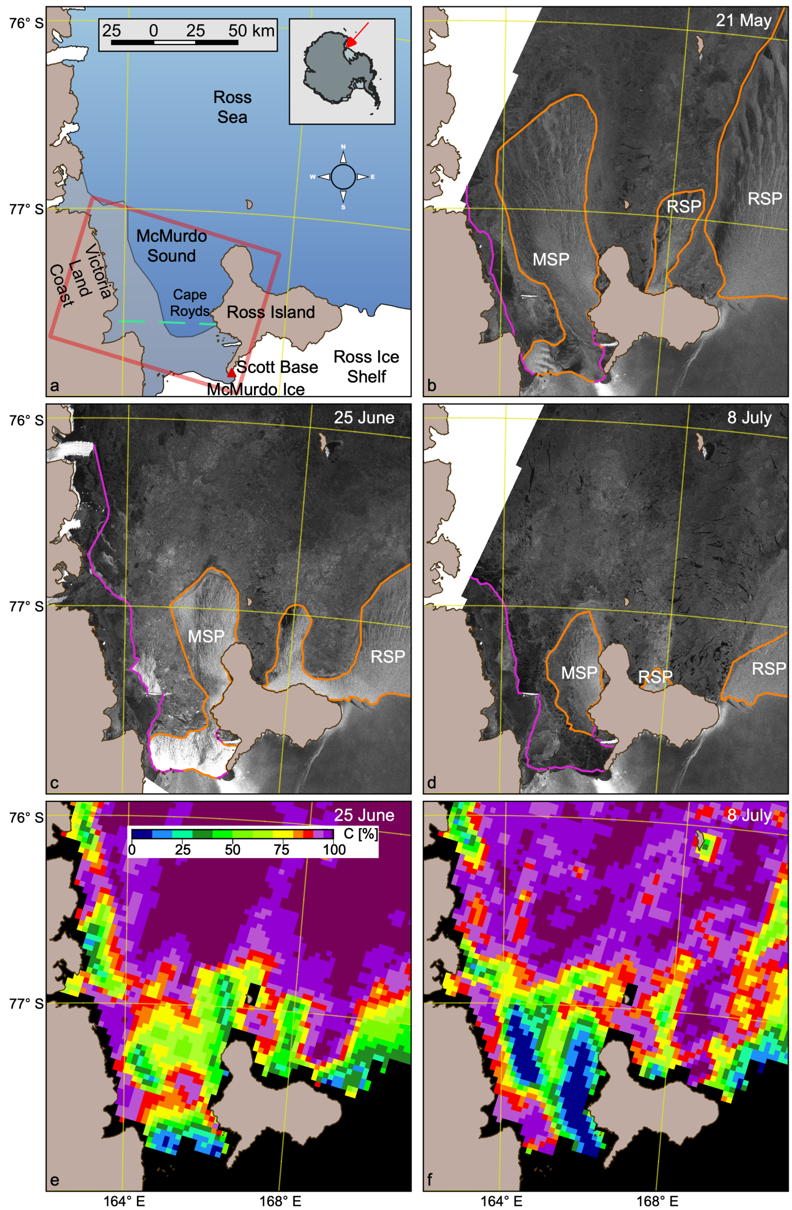

Figure 1. (a) McMurdo Sound study region, inset shows the location in the Western Ross Sea, Antarctica. The red box indicates the area ~~from~~ for which the ~~sea ice~~ sea-ice fractions were calculated. The grey shaded area indicates ~~fast ice~~ fast-ice extent from the middle of June 2014 from Fraser et al. (2020) and the green dashed line shows the -77.6 ° S parallel. (b) Sentinel-1 SAR image from 21 May 2019, (c) 25 June 2019 and (d) 8 July 2019, with the hatched areas with the orange border indicating the active area of the McMurdo Sound Polynya (MSP) and Ross Sea Polynya (RSP) and the magenta line depicting the fast-ice edge. (e) ~~Sea ice~~ Sea-ice concentrations from 25 June 2019 and (f) 8 July 2019 from the ARTIST Sea Ice (ASI) algorithm (Spreen et al., 2008).

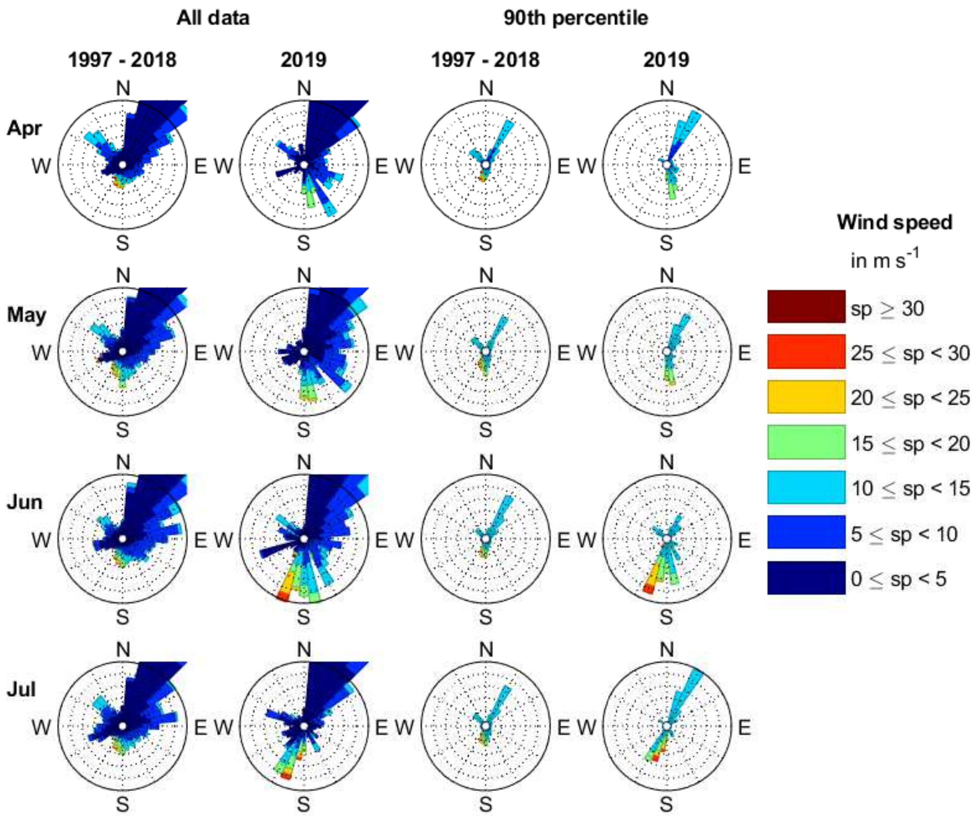

Figure 2. Wind roses ~~showing southerly winds, as recorded at the~~ constructed from Scott Base weather station data for the months of April – July~~2019.~~. The ~~left column is from~~ first and second columns show the full data set for the period ~~1998~~ 1997 – 2018 and 2019, respectively, and the ~~right column is from 2019.~~ third and fourth columns show wind speeds equal to or greater than the monthly 90th percentile for the period 1997 – 2018 and 2019, respectively. The maximum frequency shown ~~on these plots~~ is 3 %, with each circle representing an increment of 0.6 %. Note that in the first two columns the prevailing north-easterly winds extend to a maximum of 30 % (not shown) for all months.

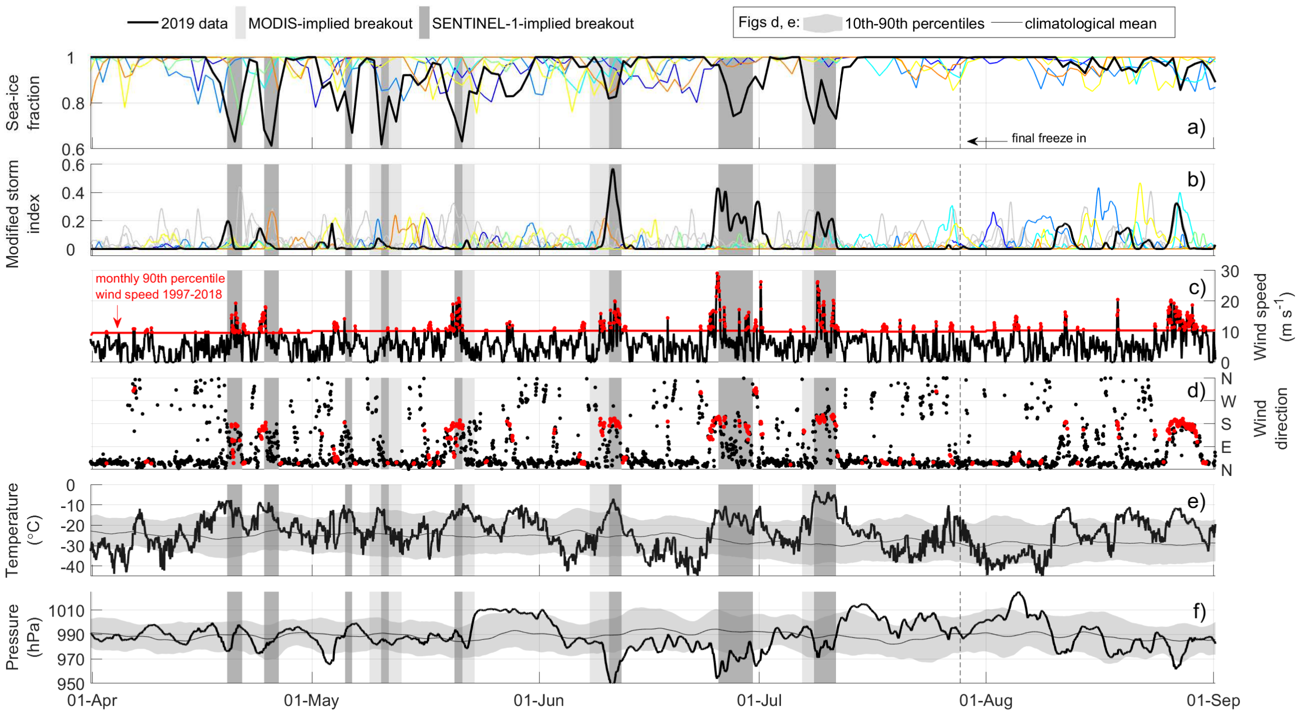

Figure 3. a) ~~Sea ice~~ Sea-ice fractional cover within the red bounding box shown in Fig. 1.a for years 2013 – 2019; ~~Bold black~~Black: 2019, coloured lines: 2013 – 2018. b) ~~Katabatic Wind~~ Modified Storm Index (~~KWI~~MSI) constructed from temperature and mean sea-level pressure anomalies for years 2002 – 2019; ~~Bold black~~ Black and coloured lines as for a), grey: years for which ~~sea ice~~ sea-ice fraction data are not available (2002 – 2012). c) ~~Southerly~~ 2019 wind speed; Red line: the monthly 90th percentile wind speed (data from ~~the Scott Base weather station~~1997 – 2018), ~~and Linda AWS (78.382 °S, 168.456 °E~~Red markers: wind speeds greater than the climatological 90th percentile. d) ~~(Lazzara et al., 2012)~~2019 wind direction; Red markers: wind speeds greater than the climatological 90th percentile. ~~d–e~~e–f) ~~Air~~ Surface air temperature and ~~mean sea level pressure~~MSLP, respectively. The 10th – 90th percentiles and climatological mean include temperature and MSLP data from ~~1996~~ 1997 – ~~2018.~~ 2018 and 2002 – 2018, respectively. Percentiles have been smoothed using a ~~24-hour~~ 3-day window. Vertical shading throughout all subplots ~~identify~~ identifies time periods where satellite products indicate fast-ice break-out events (see Section 2.1).